Cooling of Tropical Brazil (5°C) During the Last Glacial Maximum

M. Stute,* M. Forster, H. Frischkorn, A. Serejo, J. F. Clark, P. Schlosser, W. S. Broecker, G. Bonani

A 30,000-year paleotemperature record derived from noble gases dissolved in carbon-14–dated ground water indicates that the climate in lowland Brazil (Piaui Province, 7°S, 41.5°W; altitude, 400 meters) was 5.4° ± 0.6°C cooler during the last glacial maximum than today. This result suggests a rather uniform cooling of the Americas between 40°S and 40°N. A 5.4°C cooling of tropical South America is consistent with pollen records, snow line reconstructions, and strontium/calcium ratios and $\delta^{18}O$ coral records but is inconsistent with the sea-surface temperature reconstruction of CLIMAP (Climate: Long-Range Investigation, Mapping and Prediction). On the basis of these results, it appears that the tropical Americas are characterized by a temperature sensitivity comparable to that found in higher latitudes.

Whether the tropical regions were stabilized at current temperatures is a central issue in paleoclimate research. The hypothesis that the tropics may be characterized by stable temperatures rests primarily on the reconstruction of past sea-surface temperatures (SSTs) based on faunal abundances and isotopic compositions. These studies (*1–3*) indicate no or little (<2°C) change of tropical SSTs between the Holocene and the last glacial maximum (LGM). Recent support for these long-standing results comes from measurements of alkenone ratios in ocean sediments (*4*). On the other hand, continental paleoclimate records suggest that the tropics were generally significantly cooler during the LGM: snow lines and vegetation zones in the mountains near the equator appear to have been about 1 km lower during the LGM as compared to those today (*5–7*). This observation suggests that during the LGM temperatures at elevations between 2.5 and 5 km were at least 5°C lower. An increased vertical temperature gradient (lapse rate) during the LGM could potentially reconcile the different degrees of cooling of tropical oceans and continents. However, no process has yet been identified that could account for this difference in lapse rate (*5*).

We present here a continental paleotemperature record from tropical northeastern Brazil, which, because of its location at low altitude (400 m) and short distance from the coast (500 km), provides a link between continental and oceanic records. We derived paleotemperatures from the concentrations of atmospheric noble gases dissolved in ^{14}C-dated ground water. The solubility of noble gases in water is a function of temperature (*8*). The temperature under which a specific ground-water parcel was equilibrated with air can thus be determined from its noble gas concentrations (*9*).

Noble gases record the temperature at the water table where they are exchanged with the soil air. Noble gas concentrations of ground water usually exceed those calculated for thermodynamic solubility equilibrium with air in the unsaturated zone. This additional component, termed "excess air" (*10*), is most likely the result of fluctuations in the water table trapping and partially or entirely dissolving small bubbles under increased hydrostatic pressure or surface tension. Some of the excess air may also be lost by gas exchange across the water table. This secondary gas exchange most likely depends on parameters such as aquifer matrix properties, temperature, or variability in the recharge. The rates of gas exchange of the individual noble gases decrease with molecular weight. Therefore, significant gas loss results in a fractionation of the residual excess air; that is, the noble gas concentration ratios of the remaining excess air differ significantly from those observed in atmospheric air (we observed such fractionation at more than one location).

The noble gas composition of ground water can be described by three parameters: (i) temperature, (ii) amount of excess air, and (iii) the degree of fractionation of the excess air. Four atmospheric noble gases (Ne, Ar, Kr, and Xe) are available to solve a system of equations with three unknowns; that is, one noble gas concentration can be used as a free parameter for a consistency check. Helium is not used for the determination of noble gas temperatures because of sources in the aquifer that are related to the α decay of the U and Th series elements. In suitable aquifers the derived noble gas temperatures closely reflect the mean annual ground temperature at the depth of the water table [Fig. 1; see (*11*)].

We studied ground water in the Maranhão Basin at 7°S, 41.5°W in the central part of the semi-arid Piaui Province in northeastern Brazil. A succession of coarse and fine-grained sediments there forms a system of confined and unconfined aquifers and aquitards (semipervious formations) of Devonian age dipping <1° from east to west (*12*). The deepest aquifer, the Serra Grande Formation (medium to coarse-grained, typically conglomeratic sandstone, >300 m thick) is separated from the Cabeças aquifer (typically clay-rich and silt-rich sandstone, 200 to 300 m thick) by the poorly permeable Pimenteras Formation (shales, typically silt-rich, with intercalations of silt and fine- to medium-grained sandstone, 500 m thick) (*13*). The Cabeças aquifer is confined by the Longá Formation (200 m thick, partially silty shales). The individual aquifers are interconnected and form intermediate and regional ground-water flow systems with horizontal extensions of 10 to 50 km. Typical flow velocities are about 1 m/year (*12, 13*). Recharge areas are located on plateaus at elevations of 400 to 500 m, and discharge areas are located in

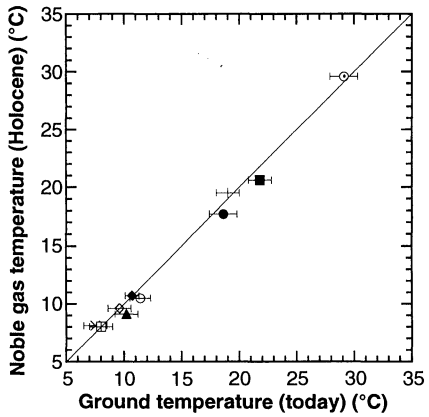

Fig. 1. Noble gas temperatures derived from ground water of Holocene age versus today's mean annual (near-surface) ground temperatures for suitable aquifers in Europe (○: Great Hungarian Plain; ◇: Bunter sandstone, United Kingdom; X: Bavaria, Germany; boxed cross: Kassel, Germany; and ◆: Bocholt, Germany), South Africa (+: Uitenhage), Brazil (⊙: Piaui), and the United States (■: Carrizo aquifer, Texas; ●: Floridan aquifer, Georgia; and ▲: San Juan Basin, New Mexico). Data points represent an average of up to 25 noble gas temperatures derived from ground water of Holocene age for each site [compiled from this study, published data (*11, 14*), as well as unpublished data]. The error in the average noble gas temperature is smaller than the symbol size.

M. Stute, Lamont-Doherty Earth Observatory of Columbia University, Palisades, NY 10964, USA.
M. Forster, Hydroisotop, 85301 Schweitenkirchen, Germany.
H. Frischkorn and A. Serejo, Universidade Federal Do Ceará, 60450 Fortaleza, Ceará, Brazil.
J. F. Clark, P. Schlosser, W. S. Broecker, Lamont-Doherty Earth Observatory of Columbia University, Palisades, NY 10964, USA, and Department of Geological Sciences, Columbia University, New York, NY 10027, USA.
G. Bonani, Institut für Mittelenergiephysik, Eidgenössische Technische Hochschule, CH-8093 Zürich, Switzerland.
*To whom correspondence should be addressed.

the low-lying river valleys at an elevation of about 150 m.

We collected 18 samples for measurement of noble gases, ^{14}C, ^{13}C, ^{2}H, ^{18}O, tritium, major ion chemistry, alkalinity, temperature, conductivity, and oxygen from both aquifers in early 1993, using standard procedures [sampling and measurement procedures are described in (*14*) and (*15*)]. We collected the samples from domestic and municipal supply wells (between 70 and 750 m deep), using installed electrical submersible pumps. We also include in our discussion the results for three samples that were obtained during an earlier sampling campaign (1985) (*13*).

The ^{14}C concentrations of the samples range from 90 pmc (pmc: percent modern carbon) to values below the detection limit (0.9 pmc). Most samples were sodium bicarbonate waters except for a few samples from the recharge areas that were dominated by calcium bicarbonate and one sample dominated by sodium sulfate (sample 17). After a steep initial increase from 0 to about 2 meq/liter, the alkalinity leveled off close to the saturation level as a function of increasing age (decreasing ^{14}C content) (Table 1). Values for $\delta^{13}C$ show a similar trend, increasing from -21 to -7 per mil (Table 1). This trend supports the notion that carbonate minerals are successively dissolving in the aquifer until saturation is reached. The concentrations of Cl^- and SO_4^{2-} do not show a systematic trend as a function of time. There is no difference in chemistry between the two aquifers except that the initial geochemical evolution seems to have occurred mainly in the Cabeças aquifer before it reaches the deeper Serra Grande aquifer. This result is consistent with hydraulic evidence suggesting that the aquifers are interconnected and that the Serra Grande aquifer, at least in some regions, is recharged through the Cabeças aquifer (*12*).

We do not include D, ^{18}O, and tritium data (<1.6 tritium units for all samples) in our discussion, because they are of limited use in tropical regions of the Southern Hemisphere. We calculated ^{14}C ages by the correction model proposed by Fontes and Garnier (*16*) (Fig. 2). This model is based on a stoichiometric balance of the dissolved carbonate species and accounts for isotopic exchange of C among soil gas, dissolved carbonate, and mineral carbonate in the saturated and unsaturated soil zones. Application of more sophisticated correction models is not appropriate, because the complexity of flow does not allow for the identification of flow paths along which geochemical evolutions of the ground water occur. However, for the following reasons the ^{14}C ages provide a reliable time scale ($\pm$ a few thousand years) for our noble gas temperature record. (i) The corrected ^{14}C ages do not strongly depend on the choice of the correction model (Fig. 2) (*17*). (ii) As discussed below, on the basis of the ^{14}C chronology, the shift in noble gas temperature occurred at about 10,000 years ago (10 ka), the time of the glacial-Holocene transition. Therefore, the intrinsic time marker of the noble gas record (the transition point between the last glacial period and the present interglacial) is in good agreement with our ^{14}C data. (iii) Radiogenic ^{4}He is produced by α decay of the U and Th decay-series elements in rocks, released into the water phase and accumulated in ground water. Therefore, ^{4}He provides an additional age indicator (*18*). Radiogenic ^{4}He concentrations (Table 2, He_{ex}) increase with ^{14}C age and cover a range typical for confined aquifers characterized by similar hydrogeologic settings and flow velocities {10^{-9} to 3×10^{-5} cm^3 [standard temperature and pressure (STP)] per gram}. (iv) The derived ^{14}C residence times in the range of 35,000 years on spatial scales between 10 and 50 km are consistent with horizontal flow velocities of roughly 1 m/year derived from a hydraulic model for

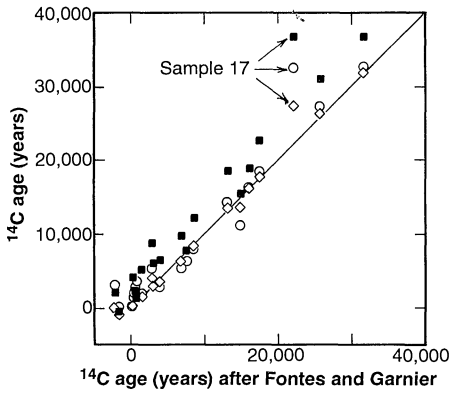

Fig. 2. Comparison of the ^{14}C ages corrected after Fontes and Garnier (*16*) used in this study with ^{14}C ages obtained from correction models (*17*) based on chemical balances (open circles, Tamers model) $\delta^{13}C$ (open diamonds, Ingerson and Pearson model), and a constant initial ^{14}C content of 85 pmc (closed squares, Vogel model).

Table 1. Selected hydrochemical data for the ground-water samples; A_0, initial ^{14}C content of the ground-water sample based on (*16*).

Sample number	Well	pH	Alkalinity (meq/liter)	ΣCO_2 (mmol/liter)	$\delta^{13}C$ (per mil)	^{14}C (pmc)	A_0 (pmc)	^{14}C age (years)
7	Project Boa Esperanca P1	5.66	0.21	1.13	−20.1	89.9	73.6	−1,650
9	Oeiras P1	6.03	0.57	1.63	−19.7	71.6	76.3	524
15	Inhuma P1	5.13	0.15	2.51	−20.7	67.7	73.8	704
18	Fazenda Montalegre	5.16	0.07	1.10	−17.0	66.2	50.8	−2,190
3	Araxa gas station	4.33	0.00	4.04	−20.5	64.5	70.8	771
13	Valenca P4	6.14	0.86	2.12	−17.9	62.9	66.6	474
8	Angical P1	7.40	1.85	1.99	−13.3	51.2	52.9	281
4	Bocaina P1	7.04	2.78	3.27	−13.8	45.1	53.7	1,450
6	San Antonio de Lisboa P1	7.00	1.75	2.09	−14.7	40.7	59.0	3,080
19	Itainopolis P2	7.25	2.41	2.68	−14.9	38.5	62.2	3,970
H10	Brejo	5.80	1.66	2.91	−19.5	32.8	82.1	7,580
2	Campestre	7.12	3.54	4.05	−11.7	29.1	41.1	2,870
H6	Tombador	8.00	1.90	1.92	−10.9	26.0	60.0	6,910
16	Santa Cruz P1	8.08	2.36	2.38	−13.4	19.5	55.3	8,620
H7	Fazenda Nova Vida	8.00	1.98	2.03	−17.1	13.1	79.0	14,800
1	Picos II	7.99	3.47	3.51	−11.8	9.1	44.8	13,100
14	Novo Oriente Saco	6.74	2.36	3.18	−15.4	8.8	61.0	16,000
23	Sao Miguel P2	7.50	2.23	2.48	−12.1	<2.0	45.2	>25,800
11	Bairo Conduru P8	8.09	3.25	3.27	−11.9	<1.3	46.1	>31,700
17	Curralinho	7.87	4.87	4.96	−6.9	<0.93	14.5	>22,100
12	Valenca P5	8.43	4.50	4.44	−8.9	<0.89	28.9	>27,800
	1σ error	±0.1	±2%	±10%	±0.1	±0.6		±3,000

parts of the area of investigation (*12*).

Typically, noble gas temperatures are determined in an iterative procedure. Initially, unfractionated air is subtracted successively from the measured concentrations, and the remaining noble gas concentrations are converted into temperatures on the basis of the solubility data and the atmospheric pressure at the elevation of the water table. This procedure is repeated until optimum agreement among the four calculated noble gas temperatures is achieved (*11*). For the Brazilian ground waters (Table 2),

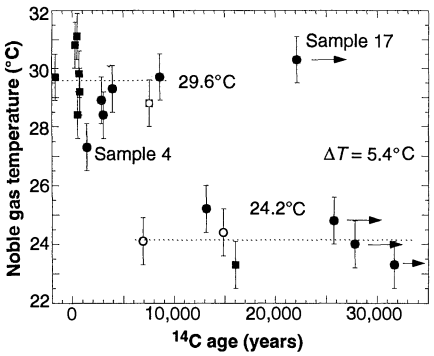

Fig. 3. Noble gas paleotemperature record derived from the Cabeças (circles) and Serra Grande (squares) aquifers in Piaui Province, northeastern Brazil. Noble gas temperatures are plotted as a function of the ^{14}C age. The arrows indicate the samples with a ^{14}C content below the detection limit. Open symbols represent samples obtained during an earlier sampling campaign (1985) (*13*). The ^{14}C ages are characterized by an error of a few thousand years because of the uncertainty of the geochemical model.

this procedure did not result in a satisfactory agreement among the noble gas temperatures derived from Ne, Ar, Kr, and Xe. We therefore assumed that some of the excess air was lost by subsequent gas evasion because of the higher partial pressure of the noble gases in the ground water as compared to the soil air. The remaining fractions of the individual noble gases X (Ar, Kr, or Xe) ($C_X/C_{X(0)}$) were approximated by a Rayleigh type formula if the remaining fraction of Ne ($C_{Ne}/C_{Ne(0)}$) is set to a fixed value:

$$\frac{C_X}{C_{X(0)}} = \left(\frac{C_{Ne}}{C_{Ne(0)}}\right)^{D_X/D_{Ne}}$$

where D_X and D_{Ne} are the temperature-dependent diffusion coefficients of noble gases in water (*19*). The amount of excess air and $C_{Ne}/C_{Ne(0)}$ were varied until optimum agreement (minimum standard deviation) among the four noble gas temperatures was achieved (Table 2).

We have checked the ability of this correction model to generate reliable noble gas temperatures by applying it to simulated noble gas concentrations based on complicated scenarios involving partial dissolution of bubbles and subsequent partial gas exchange, as well as multistage dissolution and exchange processes. Monte Carlo simulations indicate that noble gas temperatures produced by this correction model reflect the "actual" temperature at the water table with a precision of about ±0.8°C, including the measurement uncertainty. The degree of loss of excess air [1 − $C_{Ne}/C_{Ne(0)}$] does not show a trend with age. However, the remaining (fractionated) excess air, expressed as ΔNe (percent deviation from solubility equilibrium concentration) (Table 2) is roughly two to three times higher for the glacial than for the Holocene waters, a common pattern in semi-arid regions (*10*).

Except for sample 17, noble gas temperatures cluster in two groups (Fig. 3) (Table 2). The average noble gas temperature of the first group (^{14}C age less than 10,400 years) is 29.6° ± 0.3°C. The second cluster (^{14}C ages between 6,900 and >35,000 years) is characterized by an average noble gas temperature of 24.2° ± 0.3°C (errors are given as standard deviations of the mean value, $\sigma/\sqrt{N}$). The standard deviations of the clusters (σ = 0.9 and 0.7°C, respectively) are very close to the combination of the measurement precision and the excess air correction. The average noble gas temperature of the Holocene cluster, 29.6° ± 0.3°C (13 samples, except sample 4, which is a mixture of water from the Pimenteras and the Serra Grande formations), agrees well with the mean annual ground temperature in the area, 29.1° ± 1.2°C, derived from shallow ground-water temperatures as well as air temperatures. The ^{14}C (below the detection limit), δ^{13}C, and He data indicate that sample 17 is the oldest of the data set. Its high noble gas temperature suggests a formation during a warm period ≫ 35 ka.

The noble gas record (Fig. 3) suggests that the mean annual ground temperature from ≈35 ka to ≈10 ka was 5.4° ± 0.6°C

Table 2. Selected noble gas and other hydrological data for the ground-water samples. Sample locations are given in Table 1; He_{ex}: radiogenic He; $C_{Ne}/C_{Ne(0)}$: remaining fraction of Ne due to excess air after gas exchange; ΔNe:contribution of excess air to the Ne concentration normalized to the solubility equilibrium component; and T_{av}, the average noble gas temperature derived from Ne, Ar, Kr, and Xe after the optimization process.

Sample	He (cm^3 STP/g)	Ne (10^{-8} cm^3 STP/g)	Ar (10^{-4} cm^3 STP/g)	Kr (10^{-8} cm^3 STP/g)	Xe (10^{-9} cm^3 STP/g)	He_{ex} (cm^3 STP/g)	$\frac{C_{Ne}}{C_{Ne(0)}}$	ΔNe (%)	T_{av} (°C)	T_{Ne} (°C)	T_{Ar} (°C)	T_{Kr} (°C)	T_{Xe} (°C)
7	5.61×10^{-8}	2.16	2.86	5.71	7.37	7.22×10^{-9}	0.46	31.2	29.7	29.7	29.2	30.6	29.4
9	6.20×10^{-8}	2.22	2.97	5.96	7.70	1.29×10^{-8}	0.36	33.8	28.4	28.4	27.8	29.3	28.1
15	1.07×10^{-7}	2.80	3.34	6.46	7.95	5.05×10^{-8}	0.31	70	29.8	29.8	29.3	30.6	29.6
18	1.76×10^{-7}	2.22	3.00	6.02	7.51	1.30×10^{-7}	0.11	35.8	30.6	30.6	29.9	31.3	30.6
3	9.85×10^{-8}	2.73	3.25	6.24	7.83	3.91×10^{-8}	0.41	65	29.2	29.2	28.3	30.2	29.0
13	1.54×10^{-7}	2.29	3.02	6.09	7.58	1.08×10^{-7}	0.21	40.6	31.1	31.1	30.9	31.6	30.7
8	1.31×10^{-7}	2.50	3.11	6.06	7.52	7.83×10^{-8}	0.26	52.6	30.8	30.8	30.1	31.6	30.7
4	3.80×10^{-7}		3.50	6.68	8.26	2.88×10^{-7}	0.96	105.3	27.3		27.3	27.6	27.0
6	1.65×10^{-7}	3.08	3.51	6.74	8.37	1.03×10^{-7}	0.46	85.3	28.4	28.4	28.1	29.2	27.8
19	3.19×10^{-7}	2.11	2.86	5.75	7.41	2.71×10^{-7}	0.31	28	29.3	29.3	28.7	30.1	29.1
H10	1.20×10^{-7}	2.52	3.12	6.41	7.76	6.66×10^{-8}	0.36	52.2	28.8	28.8	29.3	28.1	29.1
2	8.71×10^{-8}	2.30	3.01	5.97	7.65	3.65×10^{-8}	0.36	39.2	28.9	28.9	28.3	29.8	28.7
H6	1.30×10^{-7}	3.34	3.70	7.15	9.08	5.15×10^{-8}	0.71	95.2	24.1	24.1	23.7	24.8	23.8
16	3.30×10^{-7}	2.84	3.39	6.53	8.04	2.73×10^{-7}	0.31	72.6	29.7	29.7	29.0	30.5	29.5
H7	3.83×10^{-7}	3.31	3.83	7.47	9.29	3.17×10^{-7}	0.41	93.9	24.4	24.4	24.1	24.9	24.2
1	1.83×10^{-6}	3.55	4.08	7.75	9.55	1.77×10^{-6}	0.31	108.8	25.2	25.2	24.3	26.3	24.9
14	2.13×10^{-7}	3.32	3.95	7.87	9.67	1.50×10^{-7}	0.31	93.2	23.3	23.3	23.3	23.4	23.3
23	1.30×10^{-5}	5.33	4.80	8.50	1.01	1.29×10^{-5}	0.71	213	24.8	24.8	24.4	25.6	24.3
11	1.69×10^{-6}	4.04	4.31	8.05	9.95	1.61×10^{-6}	0.46	134.4	23.3	23.3	22.5	24.3	23.0
17	3.08×10^{-5}	3.63	3.97	7.62	8.93	3.07×10^{-5}	0.31	121.2	30.3	30.3	30.7	30.6	29.7
12	5.50×10^{-6}	3.84	4.16	7.73	9.65	5.42×10^{-6}	0.46	124.3	24.0	24.0	22.9	25.4	23.7
	±2%	±1%	±0.5%	±1%	±1%	±2%		±2	±0.8				

lower than during the Holocene (*20*). We cannot exclude the possibility that the mean annual temperature may have been even lower during the glacial period for a number of reasons. (i) Aquifers tend to smooth out high-frequency fluctuations (*11*). (ii) Our record may be discontinuous, and we may have missed the coldest period. (iii) It is a matter of controversy, if during the LGM tropical South America was drier than today. The water table may have dropped as a consequence of a drier glacial climate, which would increase the temperature at the water table (temperatures in the crust typically increase at a rate of 3°C per 100 m). This would lead to an apparently lower temperature difference between present conditions and the last glacial period.

Our estimate of a 5.4°C cooling for the period between 10 and 35 ka is consistent with a ≈1000-m lowering of snow-line altitudes in the tropical mountain ranges for the LGM (*7, 21–27*). Vegetation zones in the Colombian and Ecuadorian Andes appear to have dropped by 1200 to 1500 m (1100- and 2500-m elevation, respectively) (*28–30*). The equivalent glacial cooling amounts to about 5° to 8°C if today's lapse rate is used for temperature conversion (Fig. 4). Pollen records from lowland Yucatan (100-m elevation) (*31*), lowland Panama (650-m elevation) (*32*), and southeastern Brazil (1170-m elevation) (*33*) also are consistent with a temperature change of 5° to 8°C. However, it should be noted that quantitative paleotemperature estimates derived from low-elevation pollen records are problematic. The individual temperature estimates discussed above may not be for the same time period (Fig. 4), and some estimates may be influenced by a wetter or drier glacial climate in equatorial South America. Nevertheless, available continental paleotemperature estimates provide a fairly consistent picture. General Circulation Model simulations of the glacial climate, on the other hand, cannot produce a sufficient cooling of the continents, if glacial SSTs of the CLIMAP reconstruction are used as boundary conditions (*5*).

Our noble gas record, derived from a site relatively close to the ocean and at low altitude, suggests that the CLIMAP reconstruction needs to be questioned, at least in the western equatorial Atlantic. A 5.4°C glacial cooling, as discussed here, for tropical Brazil has also been determined for the southwestern United States at a latitude of 29° to 38°N (*14, 34*) and is consistent with snow-line and vegetation zone shifts in South America at a latitude of up to 40°S (*7, 21, 25*). On the basis of this evidence, it appears that for the continental Americas the latitudinal temperature gradient during the LGM was similar to that today and that a broad zone from 40°S to 40°N had cooled more or less uniformly by at least 5°C.

Whether this statement can be extended to the adjacent oceans is still an open question. However, the results of earlier glacial SST reconstructions have recently been challenged on the basis of new oceanographic data (*4, 35, 36*). Data on Sr/Ca ratios and $\delta^{18}O$ from Barbados corals suggest a SST change of about 5°C at 15 ka (*35*). On the basis of the combined evidence, it seems possible that the glacial tropical oceans bordering the Americas have been significantly cooler than they are today. However, the serious disagreement between paleotemperature estimates based on noble gases and Sr/Ca ratios on the one hand and on O isotopes and alkenones on the other hand obviously requires further basic research on each of the methodologies used to derive paleotemperature records.

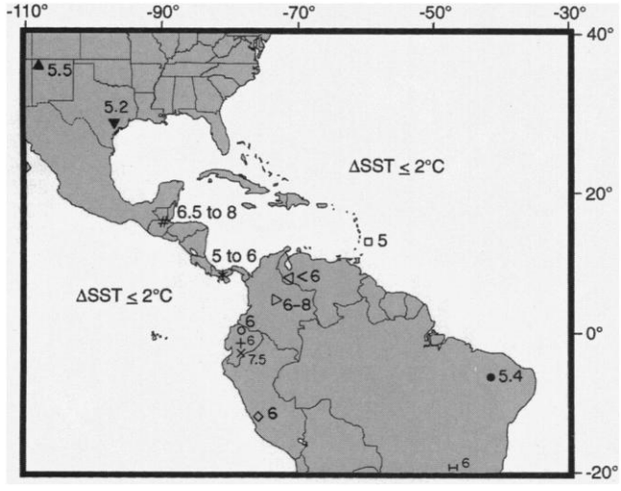

Fig. 4. Temperature differences (in degrees Celsius) between the present interglacial and the last glacial period (35 to 10 ka) derived from oceanic and continental paleotemperature records discussed in the text. The symbols mark the individual sites. The method, time period for the temperature estimate based on radiocarbon ages, and references are given below. ●: noble gases (10 to 35 ka) this study; □: Sr/Ca ratios and $\delta^{18}O$ of Barbados corals (15 ka) (*35*); ≠: pollen data, Yucatan Peninsula (14 to 24 ka) (*31*); ○: snow lines, equatorial Andes, Ecuador (14 to 34 ka) (*7, 26, 27*); *: pollen data, Panama (10 to 14 ka) (*32*); ▷: pollen data (13 to 21 ka) (*29*) and snow lines (14 to 20 ka) (*23, 24*), Cordillera Central, Colombia; X: pollen data, San Juan Bosco site, Ecuador (30 to 33 ka) (*30*); +: pollen data, Mera site, Ecuador (26.5 to 33.5 ka) (*28, 30*); ◇: snow lines, Laguna Junín site, Peru (12 to 24 ka) (*22*); ◁: snow lines, Cordillera de Mérida, Venezuela (13 to 19 ka) (*26, 27*); |-|: pollen data, Serra Negra site, Brazil (14 to 32 ka) (*33*); and ΔSST: faunal abundances (18 ka, CLIMAP) (*1*). The noble gas temperature records derived for Texas (▼) (*34*) and New Mexico (▲) (*14*) are also indicated.

REFERENCES AND NOTES

1. CLIMAP Project Members, *Geol. Soc. Am. Map Chart Ser. 36* (1981).
2. W. S. Broecker, *Quat. Res.* **26**, 121 (1986).
3. A. C. Mix, W. F. Ruddiman, A. McIntyre, *Paleoceanography* **1**, 43 (1986).
4. E. L. Sikes and L. D. Keigwin, *ibid.* **9**, 31 (1994).
5. D. Rind and D. Peteet, *Quat. Res.* **24**, 1 (1985).
6. W. S. Broecker and G. H. Denton, *Geochim. Cosmochim. Acta* **53**, 2465 (1989).
7. C. M. Clapperton, *Palaeogeogr. Palaeoclimatol. Palaeoecol.* **101**, 189 (1993).
8. R. F. Weiss, *J. Chem. Eng. Data* **16**, 235 (1971); *Deep-Sea Res.* **17**, 721 (1970); H. L. Clever, Ed., *Krypton, Xenon, and Radon—Gas Solubilities (Solubility Data Series 2*, International Union of Pure and Applied Chemistry, Pergamon, Oxford, 1979).
9. S. Oana, *J. Earth Sci. Nagoya Univ.* **5**, 103 (1957); R. Sugisaki, *Am. J. Sci.* **259**, 144 (1961); E. Mazor, *Geochim. Cosmochim. Acta* **36**, 1321 (1972).
10. T. H. E. Heaton and J. C. Vogel, *J. Hydrol.* **50**, 201 (1981).
11. M. Stute and P. Schlosser, in *Climate Change in Continental Isotopic Records* (Geophysical Monograph 78, American Geophysical Union, Washington, DC, 1993), pp. 89–100.
12. "Sudene, Grundlagen und Möglichkeiten der Landentwicklung im Trockengebiet des Staates Piaui/Nordost Brasilien" (in German) (final report of the German Hydrogeological Mission in Recife, Hannover, 1977).
13. B. T. Verhagen, M. A. Geyh, K. Fröhlich, K. Wirth, "Isotope hydrological methods for the quantitative evaluation of ground water resources in arid and semiarid areas" (Research report, Federal Ministry for Economic Cooperation of the Federal Republic of Germany, Bonn, 1991).
14. M. Stute, J. F. Clark, P. Schlosser, W. S. Broecker, G. Bonani, *Quat. Res.* **43**, 209 (1995).
15. ^{14}C was measured by accelerator mass spectrometry at the Eidgenössische Technische Hochschule, Zürich; ^{13}C by conventional mass spectrometry (University of Waterloo). Noble gases were measured mass spectrometrically at the Lamont-Doherty Earth Observatory; D, ^{18}O, and tritium, were measured by mass spectrometry, scintillation counting, and ion chromatography, respectively (Hydroisotop, Schweitenkirchen, Germany).
16. J. C. Fontes and J. M. Garnier, *Water Resour. Res.* **15**, 399 (1979). We used $\delta^{13}C = -25$ per mil for the soil gas and $\delta^{13}C = 0$ per mil for the dissolved aquifer carbonates. On the basis of the observed trends in $\delta^{13}C$, a $\delta^{13}C$ effect attributable to a change in vegetation cover (from C3 to C4 plants) seems unlikely. The ^{14}C model ages reflect the ages of the water only within a few thousand years.
17. E. Ingerson and F. J. Pearson Jr., in *Recent Researchers in the Fields of Hydrosphere, Atmosphere and Nuclear Geochemistry* (Nagoya University, Nagoya, Japan, 1964), pp. 263–283; J. C. Vogel, in *Isotopes in Hydrology* (International Atomic Energy Agency, Vienna, 1967), pp. 355–368; M. A. Tamers, *ibid.*, pp. 339–350.
18. T. Torgersen and G. N. Ivey, *Geochim. Cosmochim. Acta* **49**, 2445 (1985); I. W. Marine, *Water Resour. Res.* **15**, 1130 (1979); M. Stute, C. Sonntag, J. Deák, P. Schlosser, *Geochim. Cosmochim. Acta* **56**, 2051 (1992).
19. B. Jähne, G. Heinz, W. Dietrich, *J. Geophys. Res.* **92**, 10767 (1987).
20. This difference remains the same if the excess air component is assumed to be unfractionated versus atmospheric air. On average, this assumption would result in 3.5°C lower noble gas temperatures.
21. C. M. Clapperton, *Quat. Sci. Rev.* **9**, 299 (1990).
22. H. E. Wright Jr., *Geogr. Ann.* **65A**, 35 (1983).

23. K. F. Helmens, *Palaeogeogr. Palaeoclimatol. Palaeoecol.* **67**, 263 (1988).
24. D. G. Herd, *Publ. Geol. Ingeominas* **8**, 1 (1982).
25. S. C. Porter, *Quat. Res.* **16**, 269 (1981).
26. C. M. Clapperton, in *International Geomorphology*, V. Gardiner, Ed. (Wiley, London, 1987), pp. 843–870.
27. C. Schubert and C. M. Clapperton, *Quat. Sci. Rev.* **9**, 123 (1990).
28. K.-b. Liu and P. A. Colinvaux, *Nature* **318**, 556 (1985).
29. T. van der Hammen, *J. Biogeogr.* **1**, 3 (1974); ———, J. Barelds, H. De Jong, A. De Veer, *Palaeogeogr. Palaeoclimatol. Palaeoecol.* **32**, 247 (1981).
30. M. B. Bush, P. A. Colinvaux, M. C. Wiemann, D. R. Piperno, K.-b. Liu, *Quat. Res.* **34**, 330 (1990).
31. B. W. Leyden, M. Brenner, D. A. Hodell, J. H. Curtis, in *Climate Change in Continental Isotopic Records* (Geophysical Monograph 78, American Geophysical Union, Washington, DC, 1993), pp. 165–178.
32. M. B. Bush and P. A. Colinvaux, *J. Veg. Sci.* **1**, 105 (1990); M. B. Bush *et al.*, *Ecol. Monogr.* **62**, 251 (1992).
33. P. E. De Olivera, thesis, Ohio State University, Columbus (1992).
34. M. Stute, P. Schlosser, J. F. Clark, W. S. Broecker, *Science* **256**, 1000 (1992).
35. T. P. Guilderson, R. G. Fairbanks, J. L. Rubenstone, *ibid.* **263**, 663 (1994).
36. C. Emiliani and D. B. Ericson, *Geochem. Soc. Spec. Publ.* 3 (1993), p. 223.

37. This project was supported by National Science Foundation contract ATM 91-05538, Department of Energy contract 901214-HAR [National Institute for Global Environmental Change (NIGEC)], the W. M. Keck Foundation, the Lamont-Doherty Earth Observatory Climate Center, and the German-Brazilian Project "WAVE 5," Hydrology–Isotope Hydrology, contract 01-LK-930619. We are grateful to S. Drenkard for assisting in the measurements, numerous Brazilian colleagues for supporting the fieldwork, S. Porter, P. Colinvaux, and D. Peteet for discussions, and two anonymous reviewers for their comments. Lamont-Doherty Earth Observatory contribution 5371.

14 February 1995; accepted 3 May 1995

Primitive Boron Isotope Composition of the Mantle

Marc Chaussidon* and Bernard Marty

Boron isotope ratios are homogeneous in volcanic glasses of oceanic island basalts [−9.9 ± 1.3 per mil, relative to standard NBS 951 (defined by the National Bureau of Standards)], whereas mid-oceanic ridge basalts (MORBs) and back-arc basin basalts (BABBs) show generally higher and more variable ratios. Melts that have assimilated even small amounts of altered basaltic crust show significant variations in the boron isotope ratios. Assimilation may thus account for the higher boron ratios of MORBs and BABBs. A budget of boron between mantle and crust implies that the primitive mantle had a boron isotope ratio of −10 ± 2 per mil and that this ratio was not fractionated significantly during the differentiation of the mantle.

Convection in the mantle governs the heat transfer through the mantle and the exchange of matter in the lower mantle, the upper mantle, and the crust. Isotopic tracers are powerful indicators of these fluxes and provide information on the uncertain patterns of convection. The presence of variable but generally high $^3He/^4He$ ratios in oceanic island basalts (OIBs) tapping hot-spot material and of intermediate and homogeneous $^3He/^4He$ ratios in MORBs is strong evidence for a two-layered mantle structure, with more efficient convection in the upper mantle than in the lower mantle (*1*). In addition, He isotopes are unequivocal tracers of primitive mantle [He is not thought to be recycled back into the mantle (*2*)]. Largely because of analytical difficulties, B isotopes have not been used as a tracer (*3*). However, (i) B is incompatible and should provide evidence for depletion events in the mantle (*4*); (ii) B isotopes do not fractionate significantly at magmatic temperatures and should therefore reflect source compositions (*5*); (iii) B is not volatile under mantle conditions and is unaffected by degassing (*6*); and (iv) B isotopes are strongly fractionated during their transfer in seawater or crust (*7, 8*), so that they are potentially good tracers of subduction processes (*9*) and of shallow interaction between melts and crust. In this report, we present B isotope measurements of OIBs and in particular evaluate relations between $^3He/^4He$ and $^{11}B/^{10}B$ ratios. We examine the processes that control the B isotopic variations and the constraints they can pose for the origin and evolution of the different mantle reservoirs.

We measured B contents and $^{11}B/^{10}B$ isotopic ratios (Table 1) by ion probe in samples from five hot spots: Galápagos Islands, Loihi seamount (Hawaii), St. Helena Island, McDonald seamount (austral hot-spot track), and Afar hot-spot region (Gulf of Tadjoura). In addition, we studied samples from two back-arcs (Manus and Marianas basins). In all cases, only fresh submarine glassy lavas with a few phenocrysts were analyzed, and ion probe spots were carefully placed on glassy zones free of any bubbles or secondary products. For the OIB samples, we selected only samples that had already been analyzed for He (*10–12*) and that have variable $^3He/^4He$ ratios between $5R_a$ and $30R_a$.

The hot-spot lavas have very variable $\delta^{11}B$ values (*13*), between −14.6 ± 1.5 and −4.3 ± 1.5 per mil, that are generally lower than BABB $\delta^{11}B$ values, from −8.0 ± 1.5 to +7.5 ± 1.5 per mil (Table 1). The $\delta^{11}B$ values of OIBs partly overlap MORB values [from −6.5 ± 1.5 to −1.2 ± 1.5 per mil (*3*)], but this is probably largely due to secondary processes. In fact, the $\delta^{11}B$ of mantle melts, which have low B contents [generally ≤1 part per million (ppm)], may readily be modified at a magmatic stage as they interact with hydrothermally altered oceanic crust or seawater. This is due to the high $\delta^{11}B$ values and to the high B contents of seawater ($\delta^{11}B$ = +40 per mil and 4.5 ppm) and of seawater-altered oceanic rocks (*7*). These effects are clear for the Loihi and Afar hot-spot basalts.

Shallow-level assimilation of small amounts of oceanic crust that interacted with seawater at low temperatures is suggested at Hawaii from the positive correlations between B contents, H_2O contents, δD and $\delta^{11}B$ values (*3*), and from the $\delta^{18}O$ values, which range between +5.1 and +5.7 per mil (*14*). The two samples from the Loihi seamount analyzed in this study may represent a primary composition for the Hawaiian hot-spot melts because (i) they have the lowest $\delta^{11}B$ values (−9.3 and −10.6 per mil) and the lowest B contents (0.94 and 0.98 ppm) of the suite (*15*) and (ii) they have very high $^3He/^4He$ ratios of 27.2 ± 0.9 and 28.4 ± 0.5 (*12*). In fact, all the Hawaiian samples plot along a mixing curve (Fig. 1A) between this low $\delta^{11}B$ pole ($\delta^{11}B$ = −11 per mil and a B content of 0.9 ppm) and a pole enriched in B and in ^{11}B ($\delta^{11}B$ = +5.5 per mil and a B content of 8.5 ppm), which could be seawater-rich, altered oceanic crust (*3, 7, 16*).

The samples from the Afar plume also show a large range of $\delta^{11}B$ values (Table 1), between −4.3 ± 1.5 and −14.6 ± 1.5 per mil, but the lowest $\delta^{11}B$ values are associated, at variance with the Hawaiian samples, with low $\delta^{18}O$ values of +4.6 to +5.0 per mil (Fig. 1B). These low $\delta^{18}O$ values have been interpreted as resulting from the interaction of the ascending mantle melts with a basaltic crust hydrothermally altered

M. Chaussidon, Centre National de la Recherche Scientifique, Centre de Recherches Pétrographiques et Géochimiques, BP 20 54501 Vandoeuvre-lès-Nancy Cedex, France.
B. Marty, Centre National de la Recherche Scientifique, Centre de Recherches Pétrographiques et Géochimiques, BP 20 54501 Vandoeuvre-lès-Nancy Cedex, and Ecole Nationale Supérieure de Géologie, BP 452 54001 Nancy Cedex, France.
*To whom correspondence should be addressed.